Network dynamics for optimal compressive-sensing input-signal recovery

Victor J. Barranca,[1,2] Gregor Kovačič,[3] Douglas Zhou,[4,*] and David Cai[1,2,4,†]

[1]*Courant Institute of Mathematical Sciences & Center for Neural Science, New York University, New York, New York 10012, USA*

[2]*NYUAD Institute, New York University Abu Dhabi, Abu Dhabi, United Arab Emirates*

[3]*Mathematical Sciences Department, Rensselaer Polytechnic Institute, Troy, New York 12180, USA*

[4]*Department of Mathematics, MOE-LSC, and Institute of Natural Sciences, Shanghai Jiao Tong University, Shanghai, China*

(Received 4 July 2014; published 9 October 2014)

By using compressive sensing (CS) theory, a broad class of static signals can be reconstructed through a sequence of very few measurements in the framework of a linear system. For networks with nonlinear and time-evolving dynamics, is it similarly possible to recover an unknown input signal from only a small number of network output measurements? We address this question for pulse-coupled networks and investigate the network dynamics necessary for successful input signal recovery. Determining the specific network characteristics that correspond to a minimal input reconstruction error, we are able to achieve high-quality signal reconstructions with few measurements of network output. Using various measures to characterize dynamical properties of network output, we determine that networks with highly variable and aperiodic output can successfully encode network input information with high fidelity and achieve the most accurate CS input reconstructions. For time-varying inputs, we also find that high-quality reconstructions are achievable by measuring network output over a relatively short time window. Even when network inputs change with time, the same optimal choice of network characteristics and corresponding dynamics apply as in the case of static inputs.

DOI: 10.1103/PhysRevE.90.042908 PACS number(s): 05.45.−a, 87.19.lj, 07.05.Pj, 89.75.−k

I. INTRODUCTION

A rich assortment of network dynamics is determined by various classes of input signals [1–8]. Even if the input driving a network is unknown, it is sometimes possible to recover the input from the structure of corresponding network activity [9–13]. In general, when the number of agents, or nodes, in the network is significantly smaller than the number of external input components, this recovery process is considerably complicated and inherently underdetermined. However, if the input signal has certain structural properties, such recovery may still be feasible. Using *compressive sensing* (CS) theory and simulation of a network model, we explore the possibility of reconstructing such network input signals with respect to diverse network characteristics and dynamical regimes.

Giving a new procedure for accurately recovering signals with remarkably few samples, CS is a profound advancement in signal processing [14–17]. For signals with a sparse representation in an appropriate domain, CS theory reveals that the necessary sampling rate for successful signal recovery is significantly less than previously proposed by the Shannon-Nyquist sampling theorem [18]. While this decreased sampling rate requires solving an underdetermined system for signal recovery, CS theory also gives a methodology for selecting the optimal solution to this system. Applications of CS theory have been already found across a wide range of disciplines, such as biology, astronomy, network science, and imaging [19–24]. While CS theory is conventionally applied to static linear systems, our work takes a new perspective by investigating whether CS may also be useful in recovering inputs driving a network with time-evolving dynamics. In the case of this work, we consider a class of pulse-coupled networks with nonlinear dynamics and further comment on how the results may generalize to other network models. We first summarize our techniques for deriving linear input-output mappings embedded in nonlinear network dynamics and then demonstrate a method for using this linear mapping to recover network input signals with a large number of components via relatively few network output measurements. Since the existence of a linear input-output mapping is closely related to network dynamics, we further investigate what types of networks allow for successful CS input recovery. Using only a small number of measurements of the network output, we achieve high-fidelity input reconstructions for a broad class of networks with time-evolving dynamics and time-varying inputs.

Studying how the quality of the network CS reconstruction depends on network characteristics, we determine a class of networks that optimally samples and processes input signals. We identify clear network structures, including specific node connectivity, input signal strength, and input sampling that evoke dynamics capable of encoding network inputs with significantly more components than measured nodes. Using various metrics of dynamical coherence, such as power spectral density, correlation time, and network output variability, we demonstrate that networks exhibiting the largest degree of aperiodicity and variability in their dynamics most accurately transmit input signal information. In addition, we observe that for networks with inputs that slowly change over time, optimal input reconstructions can still be achieved in similar dynamical regimes. We also show that these CS reconstructions are robust to changes in network size and input noise.

The organization of the paper is as follows. In Sec. II A, we first introduce the network model that we will study in this work and then briefly review CS theory in Sec. II B. Next, we derive a linear mapping between network inputs and network outputs, which we use along with CS signal recovery

*zdz@sjtu.edu.cn

†cai@cims.nyu.edu

to reconstruct network input in Sec. II C. Using this network input reconstruction process, we investigate in Sec. III how the network dynamics and corresponding network CS signal reconstruction depend on the network structure. We study the strength of network forcing and node interactions in Sec. III A, and proceed to examine the input signal sampling in Sec. III B. Based on these considerations, we classify the corresponding network dynamics that best encode input signals in Sec. III C and examine the robustness of the network CS reconstructions in Sec. III D. We demonstrate in Sec. III E that the analogous principles apply to networks with time-evolving input. Finally, in Sec. IV, we discuss the implications of this work and possible future applications.

II. METHODS

A. Network model

We analyze the dynamics and topology of a model network of m output nodes driven by an n-component input signal, where $m \ll n$. In this case, the number of possible node output measurements will always be far smaller than that of the input components forcing the network. The problem of recovering an unknown network input using only the output of the nodes is therefore ill-posed and further complicated since the network dynamics evolve with time.

As a representative network, we consider a pulse-coupled, integrate-and-fire (I&F) network and analyze the characteristics of its nonlinear dynamics well-suited for CS-type recovery of input signals. This type of network model has been used to describe numerous systems, including heart-beat generation, gene regulatory interactions, and neuronal voltage dynamics [25–33]. For concreteness, we will use the terminology of neuronal systems to describe this network, but emphasize analogous physical descriptions could be formulated for other applications.

The membrane-potential dynamics of the ith neuron (node) is governed by the equation

$$\tau \frac{dv_i}{dt} = -(v_i - V_R) + f \sum_{j=1}^{n} B_{ij} p_j + \frac{S}{N_A} \sum_{\substack{k=1 \\ k\neq i}}^{m} A_{ik} \sum_{l} \delta(t - \tau_{kl}), \tag{1}$$

and advances from reset potential, $V_R = 0$, until arriving at the threshold potential, $V_T = 1$, at which time the neuron is said to spike or fire. At the lth time this occurs, τ_{il}, we reset v_i to V_R, and inject the currents $(S/N_A)\delta(t - \tau_{il})$ into all of its neighboring neurons, where $\delta(\cdot)$ is the Dirac δ function. To describe the network architecture, we say that the jth neuron is a neighbor of the ith neuron if a directed edge connects the ith preneuron to the jth postneuron (i.e., $A_{ji} = 1$). Thus, whenever the ith neuron fires, then the membrane potential of the neighboring jth neuron will undergo a jump of size S/N_A.

In this model, $\tau = 20$ ms is the membrane-potential timescale typical in the neuronal setting, $p = (p_1, \ldots, p_n)$ are the signal strengths forcing the network, $B = (B_{ij})$ is the connection matrix between the input signal and neurons, $A = (A_{ij})$ is the adjacency matrix among neurons, f and S are the respective overall strengths of those connections, and N_A is the number of connections between neurons. We choose parameters $n = 10\,000$, $m = 1\,000$, $S = 1$, and $f = 1$ for network simulations unless described otherwise. Thus, there is a factor of 10 more input components than neurons with this choice of network architecture, and consequently far fewer nodes available for measurement than the number of input components we ultimately seek to recover.

In determining the network topology, we choose the elements of connectivity matrix B to be independent identically distributed random variables, with each described by a Bernoulli distribution. The nonzero entries of B are of size $1/(N_B)$, where N_B is the number of connections in B. We assume that the probability of a directed connection between nodes, prescribed by A, is also determined by a Bernoulli distribution, and use the framework of matrix sparsity to characterize A and B. The sparsity of a connection matrix, denoted $s(A)$ and $s(B)$ for matrices A and B, respectively, is defined as the percentage of matrix elements with zero value. Sparsity therefore increases with the number of zero components in a matrix and provides a useful characterization of network connectivity ubiquitous in this work. We note that the notion of sparsity is closely related to the connection density of networks and their corresponding average degree. In particular, for a directed network of N nodes with adjacency matrix, G, the network connection density is $D = 1 - s(G)$, excluding self-connections, which yields the ratio of existing edges in the network to the total number of possible edges. In addition, for the same network, the average degree, the mean number of edges emanating from a node averaged over all nodes in a network, is $\langle k \rangle = (N - 1)[1 - s(G)]$. In the case of our specific network, since the connection probabilities among nodes and also the connection probabilities between nodes and input components consist of independent identically distributed random variables, the expected individual node degrees are equal to the average degree over the entire network. In general, as the sparsity of connections increases, the average degree of each node decreases. Thus, with knowledge of $s(A)$ and $s(B)$, a host of graphical descriptions of network connectivity can be determined.

With this choice of parameters and network structure, we simulate our model for a total time, t_f, with the initial voltages of all output neurons randomly distributed within the interval $[V_R\ V_T)$. To evolve the network, we use an event-driven algorithm through which neuronal spike times are analytically computed and the network state is updated with each firing event [34,35]. In measuring the output of our network, we determine the set of individual neuron firing rates, $\mu = (\mu_1, \ldots, \mu_m)$, which gives the average number of spikes per unit time for any neuron. For each static injected signal, we record neuronal firing rates for $t_f = 200$ ms, which is, for example, comparable to the timescale of human reaction to visual stimuli [36,37]. While this period of time is quite brief in the context of the timescale of this particular system, we demonstrate that it is sufficiently long for successful CS input reconstructions. We remark that for other networks, measures of output similar to firing rates can be defined and subsequently used to reconstruct a given input signal, p. We will discuss several general

assumptions that should be made about a given network for our analysis to apply later in Sec. II C. Furthermore, in the case of time-varying inputs, considered in Sec. III E, we also study how the input reconstruction quality depends on the duration of each input injection and corresponding firing rate measurements.

B. Compressive sensing

Conventional signal acquisition and reconstruction has largely been determined by the Shannon-Nyquist theorem [18], but, for a broad class of signals, CS theory demonstrates successful recovery is often possible using significantly fewer samples [14,16]. The Shannon-Nyquist theorem contends that, for an accurate reconstruction, the sampling rate of a given signal should be determined by its full range of constituent frequencies [18]. It is important to note, however, that in the appropriate domain, signals are often mostly composed of near-zero components. Therefore, a sampling rate ignoring this inherent sparsity may be too high. An n-dimensional signal is defined as k-sparse, with $k \ll n$, if the magnitude of at most k components exceed a near-zero threshold [14]. Real-world signals, such as images or sounds, are sparse in the frequency domain, and in other cases, sparse representations can also be learned for training sets of input signals [38–40].

The theory of CS asserts that if an n-component signal is k-sparse, then the number of necessary measurements for an accurate reconstruction should be proportional to k rather than n [15]. In this context, the problem of recovering an n-component signal, x, using only m measurements, where $m \ll n$, is equivalent to solving a large under-determined linear system. Sampling x with an $m \times n$ measurement matrix, R, this problem is equivalent to solving linear system, $Rx = b$.

If we seek to recover the sparsest solution as suggested by CS theory, then we must choose x with the minimal number of nonzero components while satisfying $Rx = b$. Since this problem cannot be solved in polynomial time [41], CS theory demonstrates that minimizing $|x|_{\ell_1} = \sum_{i=1}^{n} |x_i|$ yields a reconstruction equivalent to finding the sparsest x for a large class of measurement matrices [15]. This specific ℓ_1 minimization problem is equivalent to solving the linear programming problem

$$\text{minimize } y_1 + \cdots + y_n, \tag{2a}$$

$$\text{given } -y_i \leqslant x_i \leqslant y_i, \quad i = 1, \ldots, n, \tag{2b}$$

with constraint $Rx = b$, which can be solved via a variety of algorithms [42,43]. Moreover, if signal x is not sparse in the sampled domain, but is instead sparse under a transform, F, then the linear system $\phi\hat{x} = b$, where $\phi = RF^{-1}$ and $\hat{x} = Fx$, can be considered similarly.

With regard to the measurement matrix, R, CS theory demonstrates that matrices which exhibit sufficiently little correlation among their columns and approximately preserve the magnitude of sampled signals yield successful reconstructions of sparse inputs with high probability [15,17]. A large class of matrices, which typically contain independent identically distributed elements, have been proven to exhibit these properties [14,15], and it is therefore relatively straightforward to construct sampling schemes appropriate for CS signal recovery. Recently, a large class of binary measurement matrices, similar to connection matrices A and B, have been analyzed in the context of CS and have been demonstrated to well reconstruct sparse signals [44,45]. In our numerical experiments, we also observe consistent success in reconstructing images using static CS with sampling matrices analogous to the network input sampling matrix, B.

C. Compressive sensing network input signal recovery

While CS theory is typically applied to time-invariant linear systems, in the context of networks, the dynamics is often nonlinear and the measured output is also time-varying. Thus, a naive application of the basic CS theory, discussed in Sec. II B, to the network dynamics is not feasible. However, using coarse-graining methods [46–49], we can derive a nonlinear mapping from the network input signal to the network output (neuronal firing rates),

$$(fBp)_j = \frac{(V_T - V_R)}{1 - \exp\left(\frac{-1}{\tau\mu_j}\right)} - \frac{S}{N_A}(A\mu)_j, \tag{3}$$

which holds for each *individual* neuron in the network when the neuronal firing rates are sufficiently large, $\mu_j \gg 1$ for all $j = 1 \ldots m$, and the voltage jump induced by each spike is small, $\tau N_A \gg SA_{ji}$. Linearizing Eq. (3) in the high firing-rate regime, we obtain the linear input-output relationship,

$$fBp = \left(\tau\mu + \frac{L}{2}\right)(V_T - V_R) - \frac{S}{N_A}A\mu, \tag{4}$$

where L is an m-vector of ones.

For other network models, we note that analogous arguments may apply. With respect to the methodology presented in this work, we only require models for which it is possible to quantify the time-averaged output of each node and approximate the interactions between nodes as constant within a time window of interest, such as in the case of homogeneous Poisson inputs via classical kinetic theory [49,50].

Since the number of nodes in the network, m, is much smaller than the number of components of the input signal, n, the linear system Eq. (4) is clearly under-determined. However, assuming the input signal, p, has a sparse representation, Eq. (4) can be solved using CS theory. For example, if p is the vectorization of a two-dimensional image, we first compute the two-dimensional discrete cosine transform of the vectorized input, $\hat{p} = (\hat{p}_1, \ldots, \hat{p}_n) = (D \otimes D)p$. In this transformation, $\otimes$ denotes the $n \times n$ Kronecker product

$$D \otimes D = \begin{bmatrix} D_{11}D & \cdots & D_{1\sqrt{n}}D \\ \vdots & \ddots & \vdots \\ D_{\sqrt{n}1}D & \cdots & D_{\sqrt{n}\sqrt{n}}D \end{bmatrix},$$

where D is the $\sqrt{n} \times \sqrt{n}$, one-dimensional discrete cosine transform matrix with entries

$$D_{ij} = (D^{-1})^T_{ij} = \omega(i)\cos\left(\frac{(i-1)(2j-1)\pi}{2\sqrt{n}}\right),$$

$\omega(1) = (1/n)^{1/4}$, and $\omega(i \neq 1) = (4/n)^{1/4}$. Then, to recover $\hat{p}$, we consider the linear mapping equivalent to Eq. (4),

$$f \sum_{j=1}^{n} B_{ij}(D \otimes D)^{-1}_{ij} \hat{p}_j = \left(\tau \mu_i + \frac{1}{2}\right)(V_T - V_R) - \frac{S}{N_A} \sum_{\substack{k=1 \\ k \neq i}}^{m} A_{ik} \mu_k, \qquad (5)$$

and solve the optimization problem Eq. (2) under constraint Eq. (5), where $x_i = \hat{p}_i$. Finally, once we solve for $\hat{p}$, we invert the two-dimensional discrete cosine transform and the vectorization to recover the input signal.

With this procedure, we recover several sample images of various sizes and complexities in Fig. 1 with the optimal network parameter choices listed in Table I. It is important to emphasize that, in each case, the number of reconstructed input components is a factor of 10 greater than the number of neurons composing the network. Using the Frobenius norm, $\|p\| = \sqrt{\sum_i \sum_j p_{ij}^2}$, we compute the relative error of each reconstructed image, p_{recon}, defined $\|p - p_{\text{recon}}\|/\|p\|$. For each input image, we are able to render a satisfactory reconstruction, with each relative error less than 0.25. We observe that even for complex images, with sharp edges and high pixel variability, such as the cameraman depicted in Fig. 1(e), a recognizable reconstruction is still achievable, as displayed in Fig. 1(f). For comparison, in Fig. 1(g), we include a reconstruction of the cameraman image using static CS with the same number of samples as neurons in the network model. Comparing the relative reconstruction errors, listed in the caption of Fig. 1, we observe a small improvement in reconstruction quality by using static CS instead of CS with the network input-output mapping. Visually comparing the image reconstructions, we see that the recovery qualities agree quite well and thus input-information appears relatively well-preserved through network dynamics.

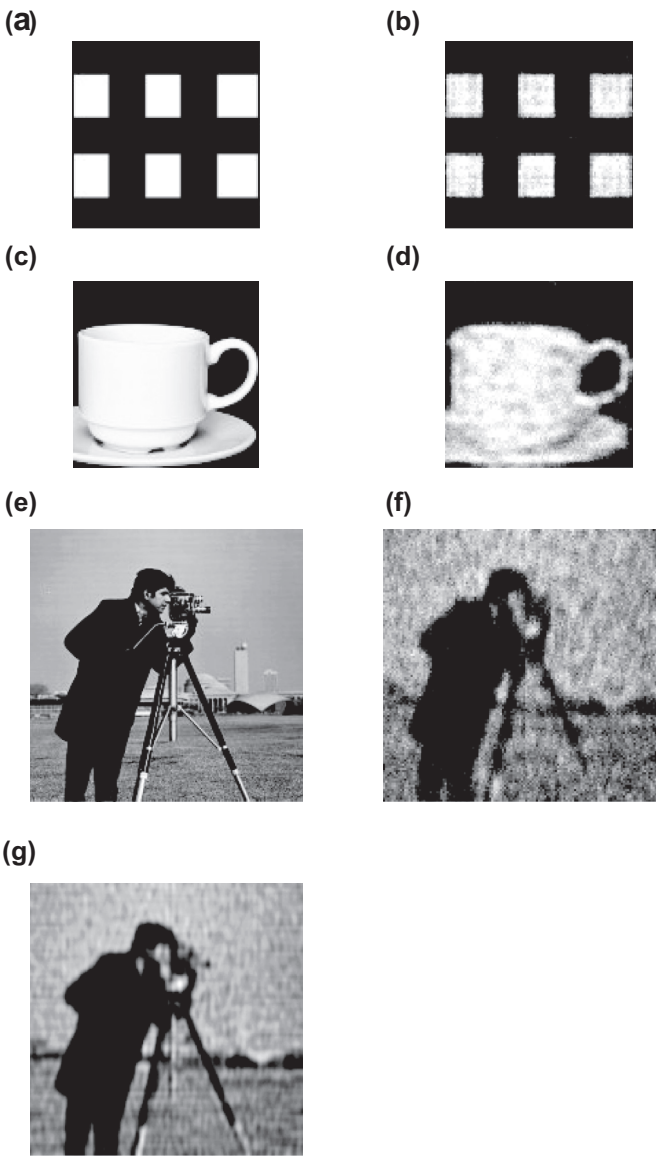

FIG. 1. Reconstruction of input images. (a), (c), (e): Original input images; (b), (d), (f): reconstructions using the network dynamics and a 10:1 input signal component to output neuron ratio, with relative errors 0.1885, 0.1756, and 0.2206, respectively. (g) Reconstruction of the image in (e) using static CS, yielding a relative error of 0.1497. Images (a) and (c) are of size 100×100 pixels, and image (e) is of size 200×200 pixels. We choose $s(A) = 0.95$, and the optimal sparsity of $s(B) = 0.999$ for reconstructions of images (a) and (c) with $n = 10\,000$ input components. For reconstructions of image (e) with $n = 40\,000$ input components, we choose the appropriate optimal sparsity of $s(B) = 0.99975$. In the reconstructions of image (e), $m = 4000$ neurons are utilized, maintaining a 10:1 ratio of input components to neurons (samples for the static CS reconstruction).

III. RESULTS

A. Input strength and output neuron interactions

To determine the network characteristics that best encode sparse inputs, we first study how the relative reconstruction error depends on the network topology and then analyze the dynamics corresponding to various levels of reconstruction quality. We begin by considering the strength of the network input and node interactions, introducing several measures of network dynamics to characterize the structure of the output underlying successful input encoding. Throughout Sec. III, we identify the impact of each network attribute by varying only one parameter at a time while holding the remaining parameters constant. In Table I, we summarize these parameter choices, which correspond to an optimal input signal reconstruction for $n = 10\,000$ input components. For each network realization, we simulate the output dynamics for $t_f = 200$ ms and fix the input signal, p.

In Fig. 2(a), we plot the reconstruction error dependence on the network input strength, f. We observe that the reconstruction is best for moderate input strengths. This corresponds to a regime in which the output neurons are then neither underdriven, such that they do not fire enough, nor driven so strongly that their interaction becomes too strong and drowns out the input signal information.

To measure the corresponding network dynamics for various choices of f, we compute the average output neuron voltage, $v(t) = (1/m)\sum_{i=1}^{m} v_i(t)$, over the time course of the simulation [51]. We observe from the average voltage plots

TABLE I. Network parameter values used in the simulation of the model network. In Sec. III, we vary only one of these parameters at a time while holding the remaining parameters constant.

Symbol	Parameter	Value
f	Input Strength	1
S	Output Neuron Connection Strength	1
$s(A)$	Sparsity of A	0.95
$s(B)$	Sparsity of B	0.999

very different averaged dynamics as a function of the input strength. If f is too small, as in Fig. 2(b), the membrane potential of a typical output neuron will approach a near-threshold value, but never spike, thereby maintaining a high average voltage. However, if the input strength is too large, as in Fig. 2(d), most output neurons will undergo rapid voltage oscillations, repeatedly spiking over small time intervals and causing high frequency average voltage oscillations. Only for a moderate input strength, such as depicted in Fig. 2(c), do these oscillations have sufficiently rich structure for an accurate input reconstruction. The nature of this structure can be further characterized by the frequency-domain representation of the average voltage dynamics and will be investigated in Sec. III C.

We find a similar relationship between optimal reconstruction quality and network dynamics in studying the reconstruction dependence on the output neuron interaction strength, S. In Fig. 3(a), we observe high-reconstruction quality for relatively small interaction strengths, with larger increases in error corresponding to higher values of S. Therefore, if the communication between the output neurons is too strong, it will likely overpower the input signal information.

We construct several raster plots to characterize the neuronal firing patterns over the duration of a simulation. A raster plot constructs a sequence of points corresponding to the index of a spiking neuron as a function of the time of the firing event. For high S, as in Fig. 3(c), we note synchronous firing events, in which large groups of output neurons typically fire at approximately the same time. However, for smaller communication strength, as in Fig. 3(d), the firing events appear relatively random and uncorrelated. Thus, it appears that more asynchronous dynamics better encode input signal information.

To complete our investigation of the effects of output neuron communication, we plot in Fig. 3(b) the reconstruction error dependence on the sparsity of A, $s(A)$, while holding the connection strength constant at $S = 1$. We observe that the reconstruction quality appears nearly independent of the sparsity of A. This indicates that output neuron communications will still not overpower the input signal strength even if there are many connections between output neurons. Since, as can be seen in Eq. (1), the communication strength is normalized by the number of connections in A, N_A, this means that whether the communication between output neurons takes the form of a few large inputs or many small inputs, the reconstruction quality is nearly unaffected when S is not large. Overall, we see that the connections between output neurons have little impact on network CS reconstructions as long as their total strength is not too large.

B. Input sampling

Considering static CS succeeds for a broad class of random sampling matrices with various sparsities [14,15],

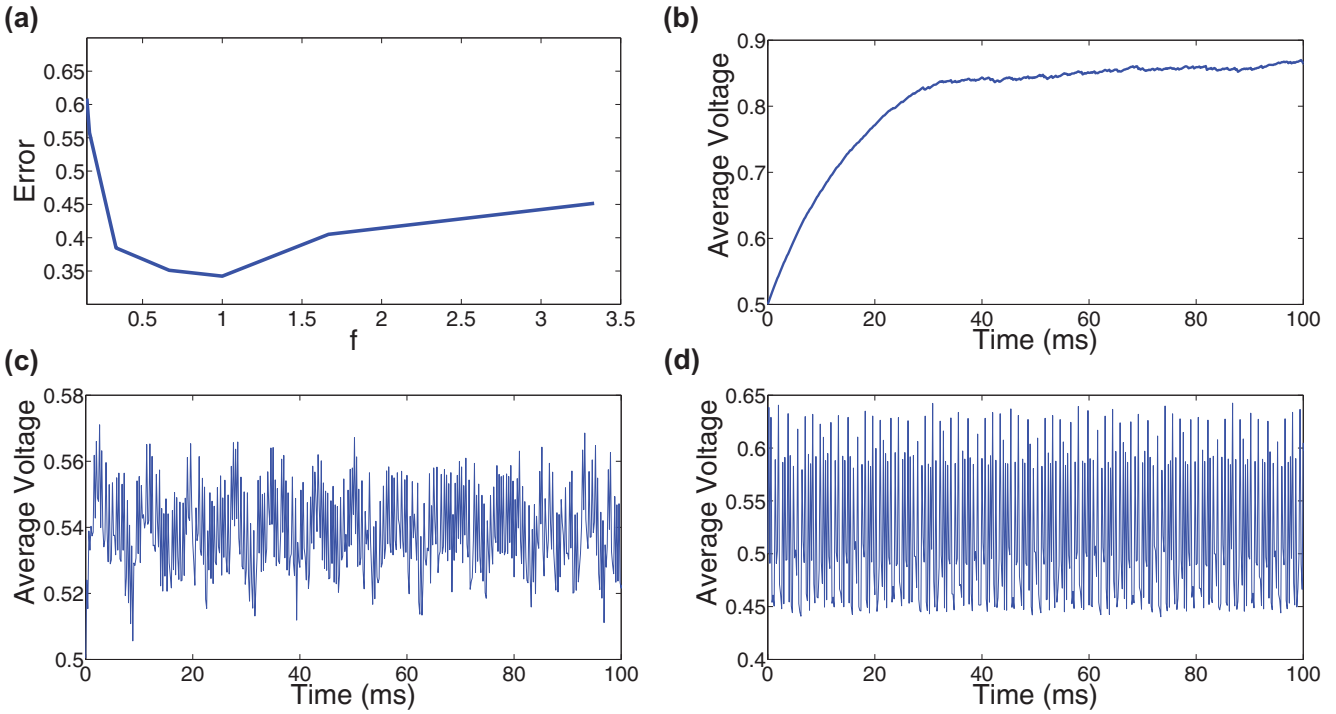

FIG. 2. (Color online) Reconstruction error and network dynamics dependence on input drive strength. (a) Reconstruction error as a function of network input strength, f. (b)–(d) Average voltage plots for $f = 0.3, 1$, and 5, respectively.

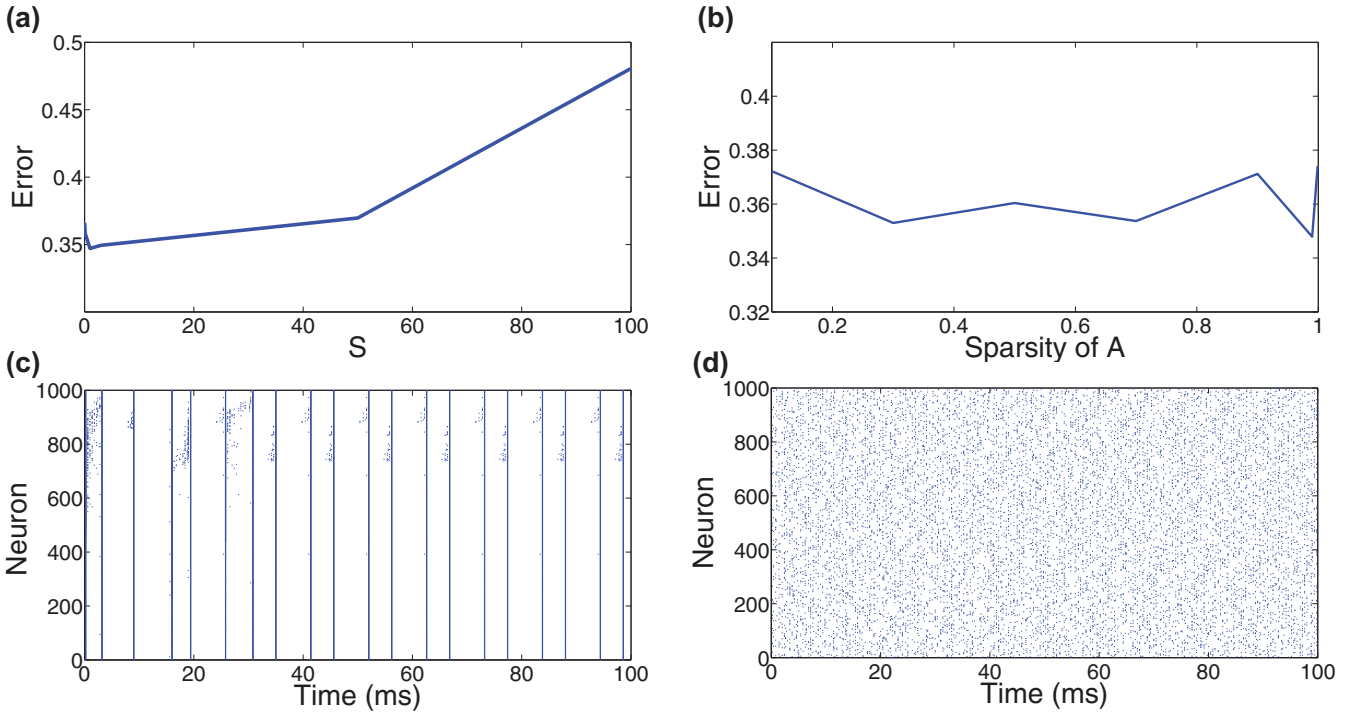

FIG. 3. (Color online) Network connectivity and interaction strength. (a) Reconstruction error as a function of neuron interaction strength S. (b) Reconstruction error as a function of the sparsity of network connectivity matrix A. (c), (d) Raster plots for $S = 1000$ and $S = 1$, respectively.

we determine if similar sampling requirements hold for network inputs reconstructed via CS. In Fig. 4(a), we plot the reconstruction error dependence on the sparsity of the signal sampling matrix, $s(B)$. In contrast to static CS, we find that connectivity of B profoundly impacts the signal reconstruction quality.

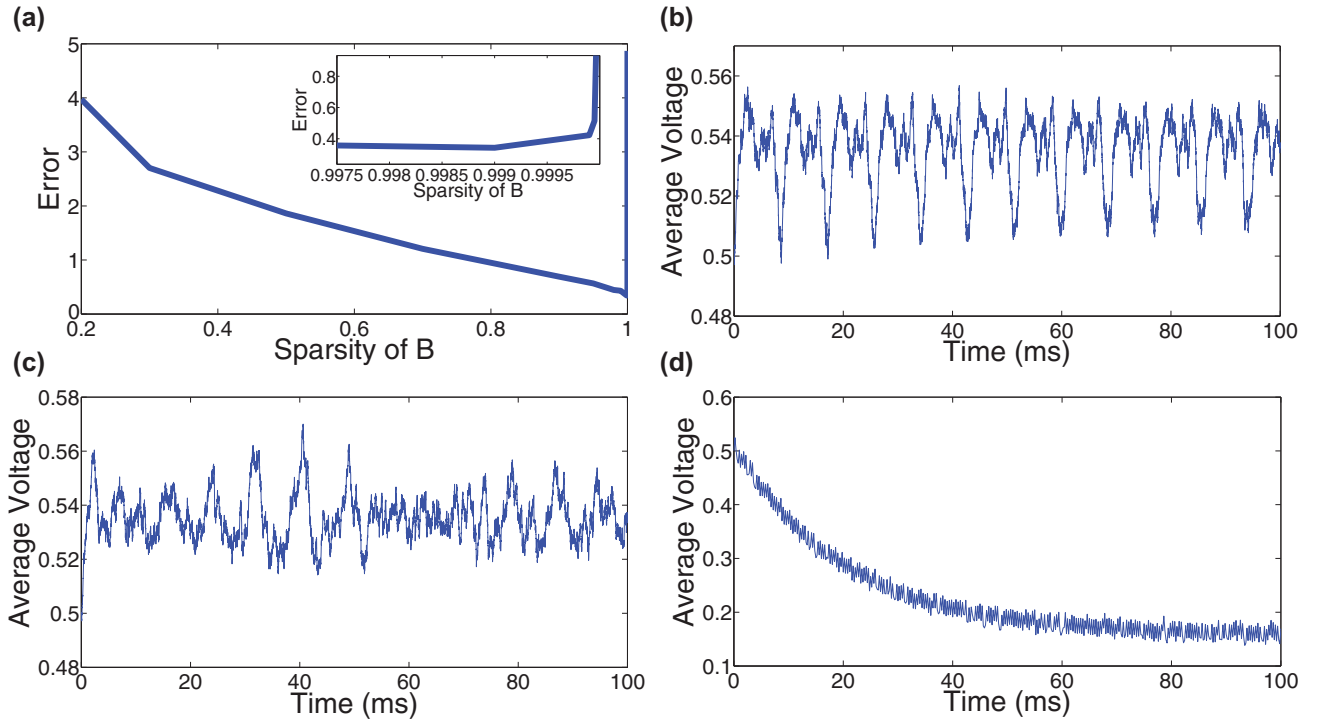

FIG. 4. (Color online) Reconstruction error and network dynamics dependence on input sampling. (a) Reconstruction error as a function of the sparsity of the signal sampling matrix, $s(B)$. Inset zooms into the highly sparse regime near $s(B) = 1$. (b)–(d) Average voltage plots for $s(B) = 0.1, 0.999$, and 0.99999, respectively.

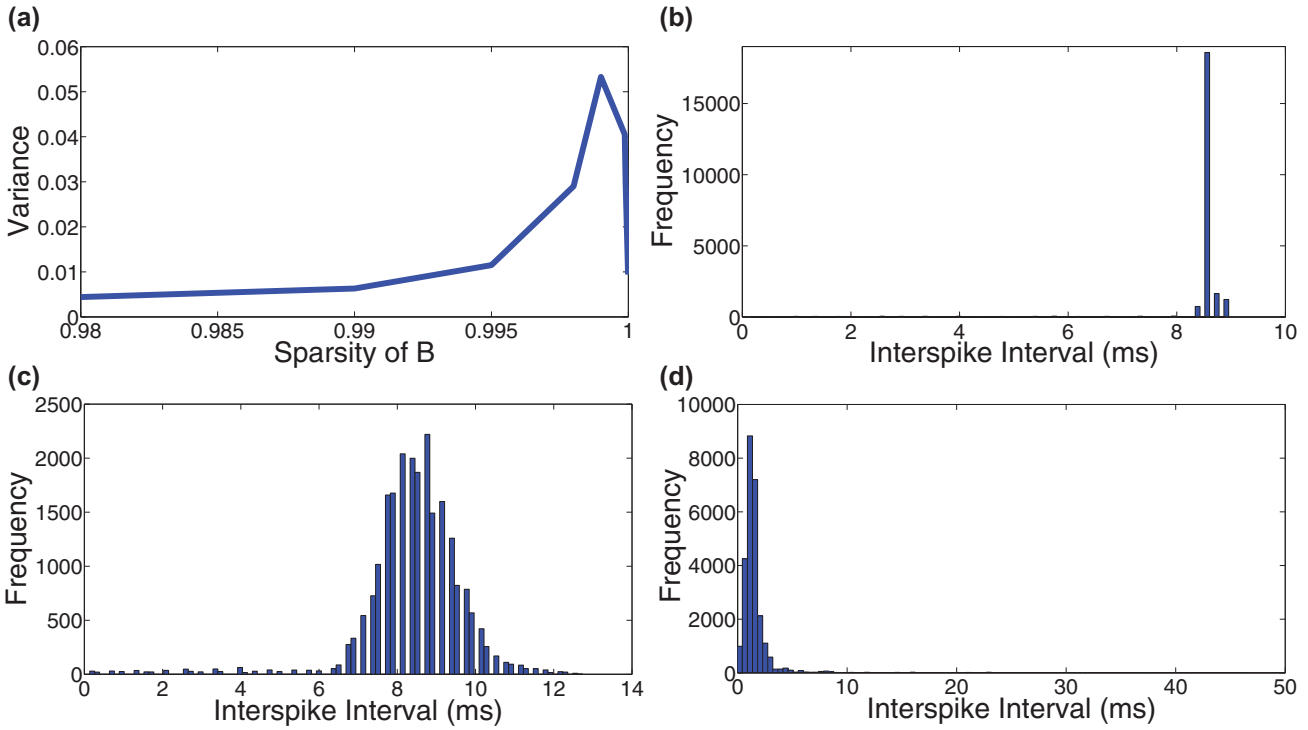

FIG. 5. (Color online) Interspike interval statistics dependence on input sampling. (a) Variance of τ_{ISI} across all firing events in the network as a function of the sparsity, $s(B)$, of input signal sampling matrix B. (b)–(d) τ_{ISI} histograms for $s(B) = 0.1$, 0.999, and 0.99999, respectively.

We observe that the reconstruction error decreases at first approximately linearly with the sparsity of B until $s(B) = 0.999$ and then sharply increases as B becomes more sparse. For sufficiently high levels of sparsity, the output neurons are not able to sample the entire input signal and therefore encode less input information in their dynamics. Similarly, for low levels of sparsity, the output neurons receive nearly the same input and are consequently unable to successfully encode different characteristics of the input signal. However, for the optimal sparsity, each input component is sampled on average once and the network output thereby encodes the maximal input information. Considering there are $n = 10\,000$ input components and only $m = 1000$ neurons in this network, the optimal sparsity corresponds to a 0.001 probability of an output neuron sampling a given input signal component. We remark that for networks with alternative numbers of nodes or input components, the optimal sparsity can be analogously identified.

Analyzing the average voltage plots in Figs. 4(b)–4(d), we observe a similar relationship between network dynamics and reconstruction quality as discussed in Sec. III A. In the over-sampled case, when $s(B) = 0.1$, the average voltage plot oscillates nearly periodically, suggesting each output neuron receives almost identical input. When the input is not sampled densely enough, only a small subset of output neurons actually samples the input and the voltages of the remaining output neurons therefore decay back to the resting voltage. Hence, the average voltage eventually oscillates around a low value, with only a subset of the input signal information encoded. For the optimal sparsity, we again observe irregular and asynchronous averaged voltage dynamics with sufficiently rich structure for successful input signal recovery.

C. Optimal network dynamics

From our investigation of the impact of network characteristics and input sampling on network dynamics, we conjecture that asynchronicity in network dynamics is a feature fundamental to successful input signal encoding and network CS reconstruction. Using several measures to quantify both the variability and periodicity in the network dynamics, we confirm our observation that optimal network dynamics are indeed highly variable and asynchronous. It appears that with this dynamical structure, the maximum input signal information is encoded and therefore available for use in the network CS reconstruction.

To quantify the variability in the output-neuron firing rates, we compute the interspike interval (τ_{ISI}) distribution. An interspike interval is defined as the period of time that elapses between two subsequent firing events for a given output neuron and is thus the multiplicative inverse of the firing rate of that particular neuron over the τ_{ISI} time interval. In Fig. 5(a), we compute the variance, $\sigma^2_{\tau_{\mathrm{ISI}}} = \langle(\tau_{\mathrm{ISI}} - \langle\tau_{\mathrm{ISI}}\rangle)^2\rangle$, of the interspike intervals over all firing events in the network as a function of the sparsity of B. We observe that the variability in τ_{ISI} sizes, and corresponding firing rates, is maximized at the optimal sparsity.

We visualize the distribution of the interspike intervals by constructing τ_{ISI} histograms in Fig. 5(b)–5(d), which plot the frequency of τ_{ISI} sizes falling into several uniformly sized bins over the set of all output neuron firing events. We note that the τ_{ISI} distribution resembles a Gaussian distribution for the optimal sparsity in Fig. 5(c). In the over-connected and over-sparse regimes, the τ_{ISI} histograms instead appear more like long-tailed and skewed Gaussian distributions with small variances. Only when the spread of the τ_{ISI} histogram is large

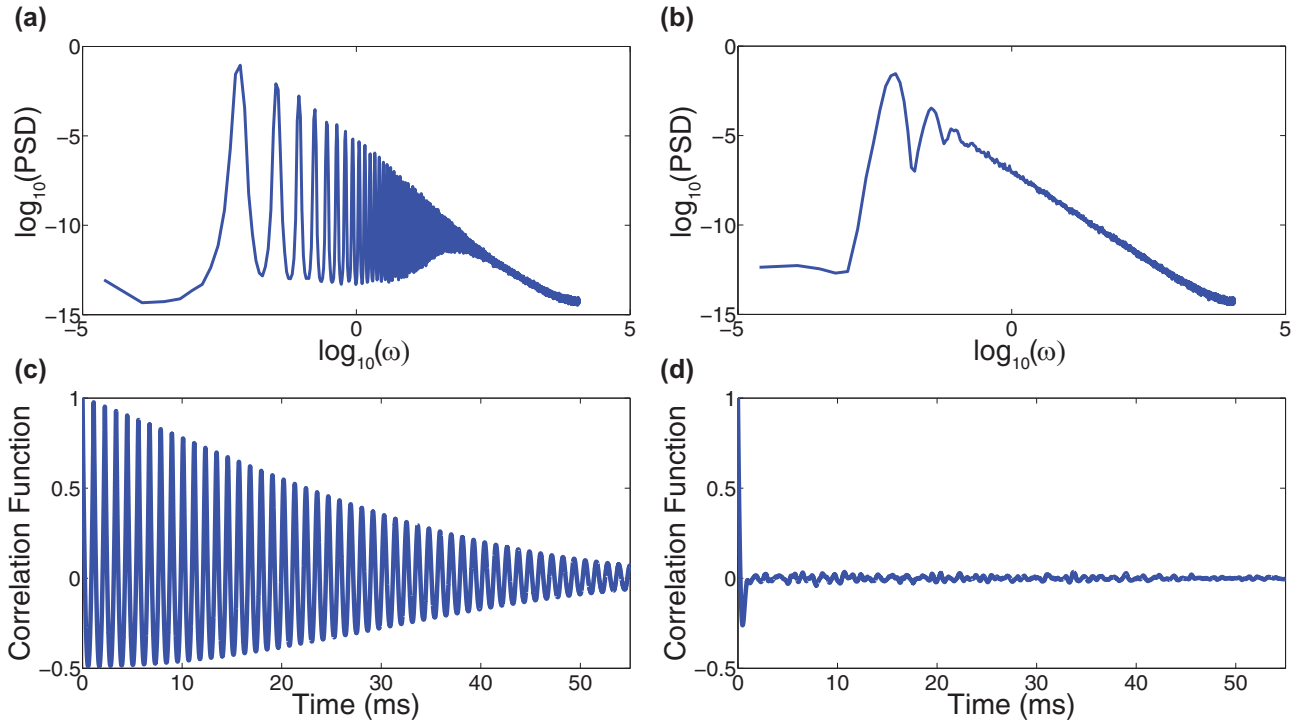

FIG. 6. (Color online) Comparison of average voltage periodicity. (a), (b) Log-log plots for the power spectral density (PSD) of the average voltage dynamics for networks with $s(B) = 0.1$ and $s(B) = 0.999$, respectively. Each PSD was computed over the course of 20 000 ms with 200 time windows. (c), (d) Correlation functions corresponding to the PSDs in considered in (a) and (b), respectively.

enough, in the Gaussian case, is there enough variation in firing patterns for a successful network CS reconstruction.

While our analysis of the τ_{ISI} variance in the time domain has made it clear that firing rate variability plays an important role in signal encoding, it does not quantify the periodicity of the network dynamics. However, as observed in Figs. 2 and 4, the network average voltage appears to demonstrate the most irregular and asynchronous dynamics in the parameter regimes for which an optimal reconstruction is achieved. We quantify the level of randomness in the network dynamics by using the spectral representation of the average voltage plot and studying the distribution of dominant frequencies as a function of the sparsity of the sampling matrix. To do this, we first compute the power spectral density (PSD) for each plot. We compute each PSD using windowing to minimize the impact of spectral leakage, a blurring of the amplitudes of signal frequency components that results from nonperiodicity over the duration of a finite sampling interval [52]. To focus on the nonzero frequency components, we initially subtract the mean value of this plot over the simulation time course from each average voltage sample before computing the PSD.

In Figs. 6(a) and 6(b), we compute the PSD log-log plots corresponding to networks with $s(B) = 0.1$ and $s(B) = 0.999$, respectively. In each case, we compute the average neuronal voltage over a long time-course of 20 000 ms and then compute the PSD using 200 time windows. In the over-connected case, corresponding to $s(B) = 0.1$, we observe an oscillatory decay, corresponding to regularly spaced PSD spikes akin to periodic dynamics. However, for the optimal sparsity of $s(B) = 0.999$, we note a linear decrease in the PSD log-log plot with a slope of approximately -2 for sufficiently high frequencies. Since the colored-noise PSD is proportional to ω^{-2} for large ω [53,54], we conclude that the network dynamics corresponding to optimal signal encoding are quite irregular and short-time correlated.

In order to quantify the randomness over a range of network topologies, we compute the average-voltage correlation function and correlation time. The correlation time gives the expected amount of time necessary for signal responses to become decorrelated and is defined as

$$T = \int_0^\infty |c(t)|\, dt, \tag{6}$$

in terms of the correlation function of the average voltage, $c(t) = R(t)/R(0)$, and autocorrelation, $R(t)$. In Figs. 6(c) and 6(d), we plot the correlation functions corresponding to the PSDs in Figs. 6(a) and 6(b), respectively. We observe that in the over-connected case, the correlation function depicted in Fig. 6(c) contains larger amplitude oscillations over a longer period of time than the correlation function in Fig. 6(d) corresponding to the optimal sparsity. We plot the correlation time as a function of the sparsity of B in Fig. 7(a), noting a minimum at the optimal sparsity of $s(B) = 0.999$. Therefore, the averaged voltage dynamics which decorrelate in the least time yields the optimal network CS reconstruction, demonstrating the most irregular, asynchronous dynamics with the shortest correlation time.

In both the time and frequency domains, we observe the same requirement of a high degree of variability in network dynamics necessary for optimal encoding of input information. We further use the notion of entropy to characterize the information content of the output neuron interspike intervals

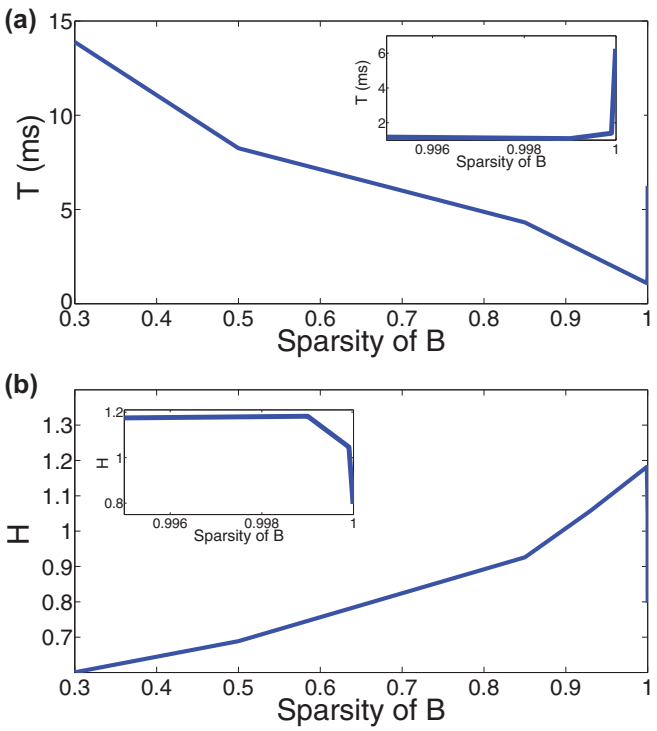

FIG. 7. (Color online) Periodicity and randomness of network dynamics. (a) Correlation time (T) as a function of the sparsity of B. (b) Entropy (H) of the interspike intervals across all network firing events as a function of the sparsity of B. Insets zoom into the highly sparse regime near $s(B) = 1$.

in our model simulations. Entropy, H, is defined as

$$H = -\sum_{\tau_{\mathrm{ISI}}} P(\tau_{\mathrm{ISI}}) \log_{10} P(\tau_{\mathrm{ISI}}), \tag{7}$$

where $P(\tau_{\mathrm{ISI}})$ denotes the probability distribution of the τ_{ISI} lengths, computed from the binned τ_{ISI} histograms collected over all firing events in a network simulation [55,56].

In Fig. 7(b), we plot the dependence of the τ_{ISI} entropy on $s(B)$. The entropy is maximized at the optimal sparsity, increasing as the correlation time of the average voltage decreases. From all of these measures, it is clear that networks whose dynamics are most asynchronous with the least correlation time encode the largest amount of information about the input signal and therefore yield the most successful network CS signal reconstructions. While network topologies evoking less asynchronous dynamics may still well encode an input signal, we observe the existence of a specific set of optimal networks capable of CS-type input encoding. We expect that this scenario may hold for other network models, giving a general intuition for how to select optimal parameter choices for successful CS network input recovery.

D. Robustness of CS network input reconstruction

Given a network with the optimal characteristics for successful CS input reconstructions, we now examine the robustness of input recovery with respect to several practical considerations. First, because the ratio of input components to nodes in the network will not be the same for every network,

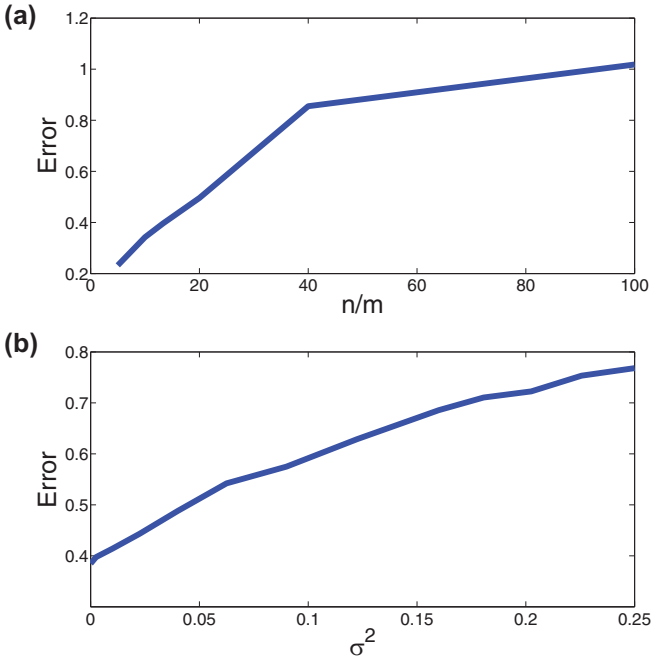

FIG. 8. (Color online) Robustness of CS network input reconstruction. (a) Reconstruction error as a function of the ratio of input components to the number of neurons in the network, n/m, for a fixed input with n components. (b) Reconstruction error dependence on the variance of injected Gaussian noise perturbing the input components.

we investigate how changes in the network size may impact the ability of network dynamics to encode inputs. In Fig. 8(a), we plot the dependence of the CS network input reconstruction error on the ratio of input components to the number of nodes in the network. As this ratio decreases, and the number of nodes in the network increases accordingly for a given input, i.e., the number of input components n is fixed, we observe a corresponding decrease in reconstruction error. Even when this ratio is as high as 30, input reconstructions are still quite accurate and capture the main features of the input. We emphasize that for each choice of network size, we adjust the network characteristics to yield optimal reconstruction quality, as described in previous sections. In addition, we expect that for increasingly large inputs, which may exhibit additional sparsity, yet larger ratios may yield viable reconstructions.

Considering many realistic input signals may be subject to noise in either their sampling or processing, we examine the effect of noise on the CS network recovery accuracy. For each node in the network, we add to the input generated from the sampled signal a perturbation in the form of Gaussian noise, $\mathcal{N}(0,\sigma^2)$, with 0 mean and variance σ^2. Note that the noise injected into each node is an independent identically distributed random variable and we choose the noise to have mean 0 so as to not statistically distort the mean input into the network. In Fig. 8(b), we depict the impact of the variance of the noise on the CS network input reconstruction error. We observe an approximately linear and relatively smooth increase in the reconstruction error with respect to the noise variance, which yields recognizable reconstructions for variances up to approximately 0.1. Considering the total

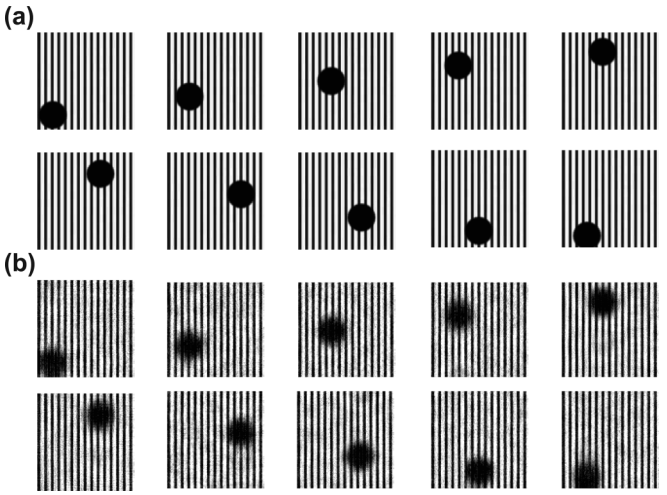

FIG. 9. Reconstruction of smoothly changing input. (a) Sequence of input image frames, each injected into the network for $t_f = 200$ ms each. (b) Network CS reconstruction of the images depicted in (a). The average reconstruction error is 0.1678.

input into each node is $\mathcal{O}(1)$, such a variance is relatively high and thus the network input recovery is quite robust to noisy inputs. In the next section, we will also demonstrate that the network input reconstructions are successful over relatively small time-scales even when the input changes with time.

E. Time-evolving input reconstructions

Measuring the robustness of our network CS reconstructions for other classes of input signals, we conclude by considering the recovery of inputs that vary in time. Can each input be encoded through network dynamics quickly enough for a successful network CS reconstruction? To answer this question, we first change the network input every $\zeta = 200$ ms while measuring the network output over the entire simulation time, t_f. Partitioning our firing rate observations into $\gamma = t_f/\zeta$ sets, corresponding to the time-course of each signal injection, we solve a total of γ network CS recovery problems.

First, in Fig. 9(a), we consider a smoothly changing sequence of ten images, processed for $t_f = 200$ ms each, depicting a moving dot on a striped background. In this case, each image is a small perturbation of the previous image, and therefore subsequent images are correlated. For correlated images, we expect that the corresponding network dynamics may be similar and therefore the network may be able to encode signal changes over small time scales. We observe in Fig. 9(b), that the reconstruction quality for each image is comparable to a network CS reconstruction of a single image.

If the input signals are instead uncorrelated, will the network be able to switch dynamical states quickly enough to encode the various inputs? We reconstruct in Fig. 10(a) a sequence of three uncorrelated images, which are each processed for the same period of time as the smoothly changing inputs. For each image we observe a similar reconstruction quality as in the case of the smoothly changing images.

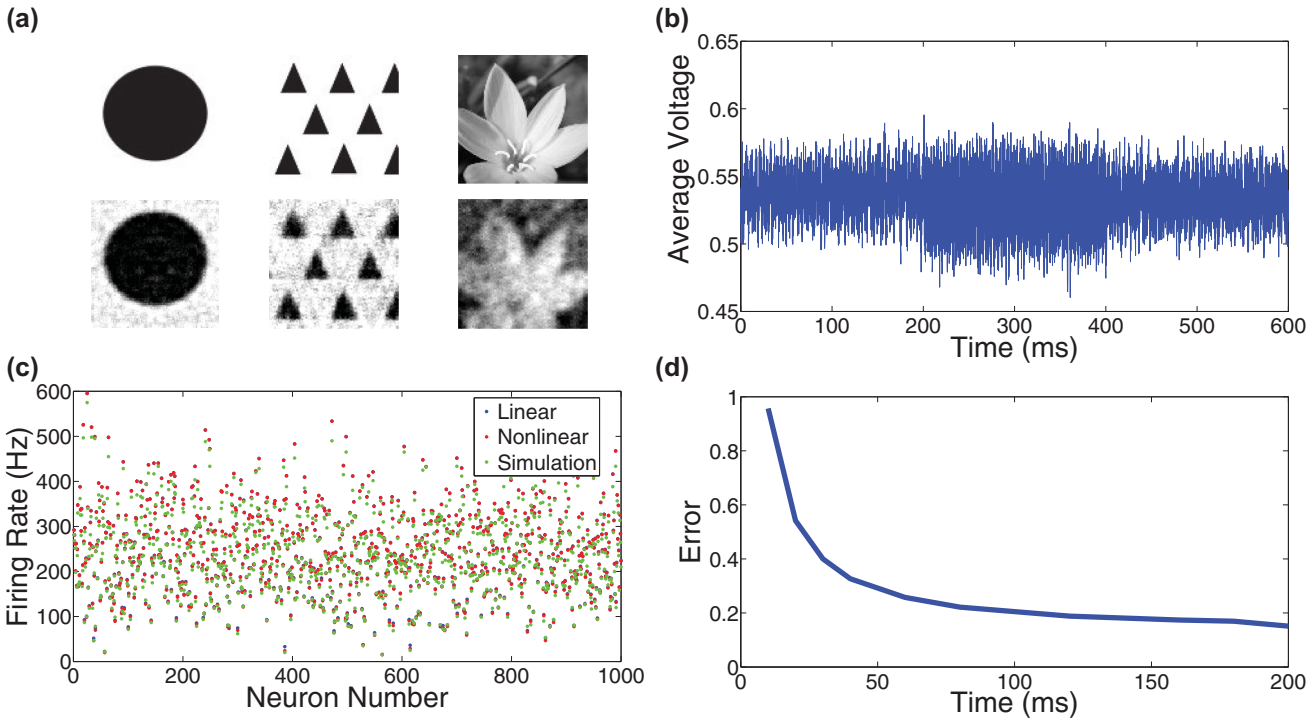

FIG. 10. (Color online) Reconstruction and dynamics for nonsmoothly changing input. (a) Top: Sequence of injected image frames. Bottom: Reconstruction of images for an injection time of $t_f = 200$ ms each. The average reconstruction error is 0.1512. (b) Average voltage plot for the network over the time course of the injection of the images in (a). (c) Firing rate agreement between the prediction of the linear mapping given by Eq. (4) (blue), prediction of the nonlinear mapping given by Eq. (3) (red), and the simulated network (green) averaged over the entire time-course of the simulation. In each case, we note that there is close agreement between the firing rates of individual neurons, with many overlapping points. (d) Reconstruction error as a function of the duration of each image injection following the initial image.

Since the average grayscale of the images is quite variable, we observe quite different average voltage magnitudes in Fig. 10(b), depending on which image is injected. However, we do see that for the same optimal parameter choices as discussed previously, each segment of the average voltage plot, corresponding to a different input image, still looks very aperiodic. Thus, even for dynamic inputs, similar types of network dynamics still appear optimal for network CS input recovery. Averaging the neuronal firing rates over the entire duration of simulation, we observe in Fig. 10(c) that, neuron-by-neuron, the simulated neuron firing rates and theoretical firing rates computed using Eqs. (3) and (4) agree very well.

Considering that the network CS reconstruction quality for even a sequence of uncorrelated images is comparable to that of a single image, we finally investigate the minimal time that each input signal must be processed for a viable reconstruction. We inject the initial signal in Fig. 10(a) for the full 200 ms timescale and then use a decreased processing time for the subsequent signals.

In Fig. 10(d), we plot the dependence of the average reconstruction error on the length of time each subsequent image is processed through network dynamics. We find that as long as the input is injected for at least approximately 80 ms, a sequence of highly accurate reconstructions is achievable with only small improvements in reconstruction quality for longer processing times. For small input durations, the error increases rapidly with shortening injection times, suggesting that the dynamics have not had sufficient time to encode the input information. We remark that we observe the same trend in the case of correlated images, such as those depicted in Fig. 9(a). With respect to the membrane-potential time-scale chosen for our particular network, such input processing times are particularly brief considering they are of the same order of magnitude as typical human reaction times [36,37], and we expect similarly rapid processing times will generalize to other network applications. It is noteworthy that even with such drastic changes in input, the network dynamics are still able to encode signal information over short timescales. Hence, CS via network dynamics appears feasible also in the case when both the network inputs and outputs are time-evolving as long as the rate of change of the input is not too high.

IV. DISCUSSION

Through an investigation of the impact of both network characteristics and corresponding dynamics on the quality of network-input reconstructions, we determined that variability in the network output is a key feature necessary for successfully encoding input information. Driving our model network with inputs that have many more components than network nodes, we were able to use CS theory combined with an intrinsic linear input-output mapping to recover network inputs with many more components than network nodes. The quality of the input reconstructions heavily depended on network features, such as the interactions between nodes and the sampling of the input signal, but for an optimal choice of parameters, we were able to consistently obtain accurate reconstructions.

Analyzing the network dynamics underlying the quality of the CS reconstructions, we applied several measures of variability and periodicity to the network activity, which all affirmed that highly variable network-output is a guiding feature for optimal input information transmission. While we expect the same relationship to hold for other networks, it would be interesting to test this theory in other contexts and determine to what extent the optimal network dynamics are similar.

In the case of time-evolving inputs, our theory of network CS reconstruction and corresponding dynamics appears robust as long as each input is processed for a sufficiently long period of time. We expect that the duration of the input sampling should depend on the complexity of the input signal or its sparsity in the appropriate domain, but a more systematic investigation is necessary to verify this hypothesis. Using classical CS probabilistic arguments combined with dynamical systems theory, it may also be possible to quantify the exact dependence of the required sampling duration on signal features.

While we have applied our theory to a model network, we expect that a similar relationship between the variability of network dynamics and quality of a network CS reconstruction to hold in the case of real-world systems. Information theory demonstrates that more random-like system outputs encode more information about a given input [55,56]. Therefore, we posit that a similar principle should underline information encoded through network dynamics and corresponding network CS signal recovery. For real-world, time-evolving networks with highly unpredictable output, we anticipate that CS should be highly useful in recovering unknown input signals using very few output measurements.

ACKNOWLEDGMENTS

The work was supported by Grants No. NSF DMS-0636358 (for V.B.), the Shanghai Pujiang Program No. 10PJ1406300, National Science Foundation in China No. NSFC-11101275 and No. 91230202, and the Scientific Research Foundation for the Returned Overseas Chinese Scholars from State Education Ministry in China (for D.Z.), No. NSF DMS-1009575, Shanghai No. 14JC1403800 (D.C., D.Z), and the NYU Abu Dhabi Institute No. G1301.

[1] B. Hassard, J. Theor. Biol. **71**, 401 (1978).
[2] V. J. Barranca, D. C. Johnson, J. L. Moyher, J. P. Sauppe, M. S. Shkarayev, G. Kovačič, and D. Cai, J. Comput. Neurosci. **37**, 161 (2014).
[3] S. Strogatz, Nature **410**, 268 (2001).
[4] S. N. Dorogovtsev and J. F. F. Mendes, Adv. Phys. **51**, 1079 (2002).
[5] M. Newman, SIAM Rev. **45**, 167 (2003).
[6] S. Boccaletti, V. Latora, Y. Moreno, M. Chavez, and D.-U. Hwang, Phys. Rep. **424**, 175 (2006).
[7] A. Barrat, M. Barthélemy, and A. Vespignani, *Dynamical Processes on Complex Networks* (Cambridge University Press, Cambridge, New York, 2008).
[8] G. Buzsaki and A. Draguhn, Science **304**, 1926 (2004).

[9] M. Patel, A. V. Rangan, and D. Cai, J. Comput. Neurosci. **27**, 553 (2009).
[10] G. Laurent, Trends Neurosci. **19**, 489 (1996).
[11] J. M. Goncalves and S. Warnick, IEEE Trans. Automat. Contr. **53**, 1670 (2008).
[12] D. D. Feng, K.-P. Wong, C.-M. Wu, and W.-C. Siu, IEEE Trans. Info. Technol. Biomed. **1**, 243 (1997).
[13] R. E. Kalman, Trans. ASME J. Basic Eng. **82**, 35 (1960).
[14] E. J. Candes, J. K. Romberg, and T. Tao, Commun. Pure Appl. Math. **59**, 1207 (2006).
[15] E. J. Candes and M. B. Wakin, IEEE Signal Process. Mag. **25**, 21 (2008).
[16] D. L. Donoho, IEEE Trans. Info. Theory **52**, 1289 (2006).
[17] R. Baraniuk, IEEE Signal Process. Mag. **24**, 118 (2007).
[18] C. E. Shannon, Proc. IRE **37**, 10 (1949).
[19] M. Lustig, D. Donoho, and J. M. Pauly, Magn. Reson. Med. **58**, 1182 (2007).
[20] W. Dai, M. A. Sheikh, O. Milenkovic, and R. G. Baraniuk, EURASIP J. Bioinform. Syst. Biol. **2009**, 162824 (2009).
[21] M. A. Herman and T. Strohmer, Trans. Signal Process. **57**, 2275 (2009).
[22] J. Bobin, J.-L. Starck, and R. Ottensamer, J. Sel. Topics Signal Process. **2**, 718 (2008).
[23] W.-X. Wang, Y.-C. Lai, C. Grebogi, and J. Ye, Phys. Rev. X **1**, 021021 (2011).
[24] W.-X. Wang, R. Yang, Y.-C. Lai, V. Kovanis, and C. Grebogi, Phys. Rev. Lett. **106**, 154101 (2011).
[25] C. S. Peskin, *Mathematical Aspects of Heart Physiology* (Courant Institute of Mathematical Sciences, New York, 1975), pp. 268–278.
[26] J. Honerkamp, J. Math. Biol. **18**, 69 (1983).
[27] W. Mather, M. R. Bennett, J. Hasty, and L. S. Tsimring, Phys. Rev. Lett. **102**, 068105 (2009).
[28] A. N. Burkitt, Biol. Cybern. **95**, 1 (2006).
[29] R. E. Mirollo and S. H. Strogatz, SIAM J. Appl. Math. **50**, 1645 (1990).
[30] D. Somers, S. Nelson, and M. Sur, J. Neurosci. **15**, 5448 (1995).
[31] Z. Wang, Y. Ma, F. Cheng, and L. Yang, Image Vision Comput. **28**, 5 (2010).
[32] D. Cai, A. Rangan, and D. McLaughlin, Proc. Natl. Acad. Sci. USA **102**, 5868 (2005).
[33] D. Zhou, A. V. Rangan, D. W. McLaughlin, and D. Cai, Proc. Natl. Acad. Sci. USA **110**, 9517 (2013).
[34] R. Brette, M. Rudolph, T. Carnevale, M. Hines, D. Beeman, J. M. Bower, M. Diesmann, A. Morrison, P. H. Goodman, F. C. Harris Jr., M. Zirpe, T. Natschlager, D. Pecevski, B. Ermentrout, M. Djurfeldt, A. Lansner, O. Rochel, T. Vieville, E. Muller, A. P. Davison, S. E. Boustani, and A. Destexhe, J. Comput. Neurosci. **23**, 349 (2007).
[35] K. A. Newhall, G. Kovačič, P. R. Kramer, and D. Cai, Phys. Rev. E **82**, 041903 (2010).
[36] K. Amano, N. Goda, S. Nishida, Y. Ejima, T. Takeda, and Y. Ohtani, J. Neurosci. **26**, 3981 (2006).
[37] S. Ando, Y. Yamada, and M. Kokubu, J. Appl. Physiol. **108**, 1210 (2010).
[38] D. J. Field, Neural Comput. **6**, 559 (1994).
[39] M. Zibulevsky and B. A. Pearlmutter, Neural Comput. **13**, 863 (2001).
[40] R. Rubinstein, A. M. Bruckstein, and M. Elad, Proc. IEEE **98**, 1045 (2010).
[41] A. M. Bruckstein, D. L. Donoho, and M. Elad, SIAM Rev. **51**, 34 (2009).
[42] J. A. Tropp and A. C. Gilbert, IEEE Trans. Info. Theory **53**, 4655 (2007).
[43] D. L. Donoho and Y. Tsaig, IEEE Trans. Info. Theory **54**, 4789 (2008).
[44] M. A. Iwen, J. Complex. **30**, 1 (2014).
[45] R. Berinde, A. C. Gilbert, P. Indyk, H. Karloff, and M. J. Strauss, in *Proceedings of the 46th Annual Allerton Conference on Communication, Control, and Computing, 2008* (IEEE, New York, 2008), pp. 798–805.
[46] A. Treves, Network **4**, 259 (1993).
[47] R. Ben-Yishai, R. Bar-Or, and H. Sompolinsky, Proc. Natl. Acad. Sci. USA **92**, 3844 (1995).
[48] Y. Kuramoto, Physica D **50**, 15 (1991).
[49] A. V. Rangan, G. Kovačič, and D. Cai, Phys. Rev. E **77**, 041915 (2008).
[50] D. Cai, L. Tao, M. Shelley, and D. McLaughlin, Pro. Natl. Acad. Sci. USA **101**, 7757 (2004).
[51] U. Mitzdorf, Physiol. Rev. **65**, 37 (1985).
[52] F. J. Harris, Proc. IEEE **66**, 51 (1978).
[53] N. Wiener, *Time Series*, MIT Press Paperback Series (MIT Press, Massachusetts, USA, 1964).
[54] C. W. Gardiner, *Handbook of Stochastic Methods*, 3rd ed. (Springer, Berlin, 2004).
[55] F. Rieke, D. Warland, R. de Ruyter van Steveninck, and W. Bialek, *Spikes: Exploring the Neural Code*, Computational Neuroscience (MIT Press, Cambridge, 1996).
[56] I. Nemenman, W. Bialek, and R. de Ruyter van Steveninck, Phys. Rev. E **69**, 056111 (2004).